Strain and damage sensing by CNT modified adhesive films and fiber optic distributed sensing. Comparison of performances in a double lap bonded joint.

Alfredo Güemes[1], Angel Renato Pozo-Morales[1], Antonio Fernandez-Lopez[1], Xoan F Sánchez-Romate [2], Maria Sánchez [2], Alejandro Ureña [2]

[1] Lab of Composites and Smart Structures, Dpt Aeronautics, Univ Politecnica Madrid, Spain;
[2] Materials Science and Engineering Area, Universidad Rey Juan Carlos, Móstoles (Madrid), Spain
*corresponding author, E-mail: alfredo.guemes@upm.es

Abstract

Bonded joints show a complex stress field, with large strain gradients, usually mainly known by numerical models. Experimental measurements are obtained at this paper, and the feasibility and performances of two low intrusivity sensing techniques are compared. The properties of CNT doped adhesive films are well known for uniform strain field; by plotting conductive patterns on the film, the response at high and low shear strain regions is also obtained, affording a much better insight on the possibilities of this technique. An optical fibre embedded into the adhesive film, aligned to the loads, experience the strong strain gradients that are predicted by the models. Experimental results are compared to the numerical predictions given by Volkersen shear-lag model.

1. Introduction

There is a very large amount of references related to bonded joints, which is indicative of the interest of the topic. Ref [1] gives a survey of more than 200 articles published from 2009 to 2016, while Ref [2] gives the references from a former period. Most of the articles are dealing with stresses modeling, either by analytical or by numerical FEM methods. In the latest years the attention is focused on the strength prediction, by using the Cohesive Zone Model (CZM).

The models predict that shear stresses distribution is strongly non-uniform along the joint length, peaking at both ends. Added to the low thickness of the adhesive layer, typically 0,2 mm, it makes rather difficult to obtain experimentally the strain field. Digital Image Correlation (DIC) may afford a quite detailed map of the strain field from the lateral view of the adhesive film, with quite good spatial resolution [3, 4]. The experimental shear strains obtained at Ref. [4] (averaged through the thickness) compare quite well with the predictions from the 1-D shear lag model. Ref. [5] obtained also a similar agreement between the model results compared to the experimental findings obtained by Moiré interferometry. The setup for these techniques and the associated data processing is rather complex, limiting its usage.

The low size of the optical fibre (OF), with a typical diameter of 0,15 mm, when coated with a polyimide protective layer, make it feasible to embed the fiber inside the adhesive film without disturbing the strain field. A strain sensor could have been engraved at the core of the optical fibre, called FBG (Fibre Bragg Grating), allowing the axial strain to be measured a t this point. Also, it can be multiplexed (by writing several sensors at the same optical fibre), affording a much better insight about the strain distribution. FBGs started to be used as strain sensors in the '90s, Ref. [6] was one of the earliest publications related to its usage for strain monitoring in bonded joints. Ref [7] describes quite clearly the experimental details for using this technique. A major change on the technology of fiber optic strain sensing happened at 1998 after the implementation of OFDR (Optical Frequency Domain Reflectometry), and its application for the distributed sensing [8], getting strain information all along the optical fiber, even without the need to engrave any sensor on it. Since then, a large number of articles have appeared on the topic [9 to 14], including a PhD dissertation from the University of Tokyo [15], detailing every practical aspect of the related experiments. A common limitation for former works is that, in most of the cases, tests are done on single lap bonded joints, with strong out-of-plane displacements caused by the load misalignment, which usually mask the strains caused by the shear loads. A double lap bonded joint is selected for our experiments, to avoid those bending moments.

It has been demonstrated by many authors that the electrical resistivity of carbon nanotube (CNT) thin films increases with strain, this effect can be explained by the diminution of contacts points among nanotubes network, and the role of the polymer influencing the tunneling barrier, the gap between neighboring tubes. The percolation threshold is defined as the CNT contents when the electrical conductivity of the blend increases by orders of magnitude due to the establishment of conducting paths. The sensitivity as strain sensor attains a maximum near the percolation threshold.

The threshold is dependent on the nature of CNT and resin, its functionalization, and the avoidance of agglomerates, among other parameters, and usually range

from 0,1% to 1%. Refs [16, 20] give a review of some published works on CNT doped resins, with applications on strain and damage sensing.

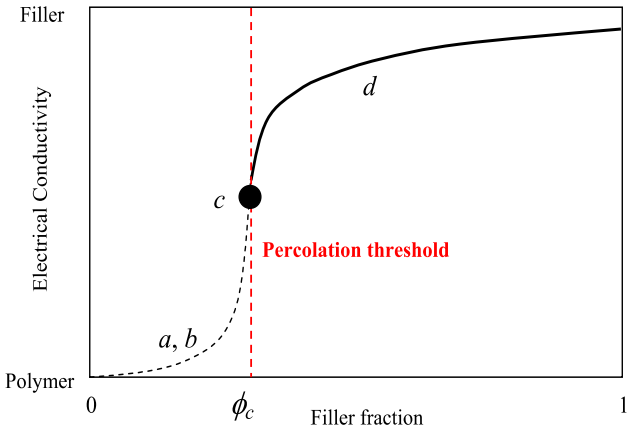

Figure 1. Conductivity of CNT doped resins (from Ref 16)

Instead of doping the resin paste, an alternative approach is to prepare a CNT dispersion on an aqueous media that can be spread onto the conventional uncured adhesive film. At a former paper [21] the optimized conditions to prepare the dispersion were discussed, and also it was demonstrated that the addition of CNTs did not have a detrimental effect on lap shear strength (LSS), with the best results being achieved in the case of dispersions about 0.25 wt%. At this work we focus on the sensitivity of this kind of sensor and its response to complex strains field.

2. Materials and manufacturing of the specimens

The dimensions of specimens to be built are sketched at Fig 2, pictures from the two sides of the specimens are also included there. One side of the specimen includes conductive strips with doped adhesive film, while the other side has one embedded optical fibre, which was included with the adhesive film before curing.

- Adherents were done with CFRP laminates, made with 13 plies of CYCOM 977-2 unidirectional tape, with a layup $[(0,90)_3,\underline{0}]s$. The basic properties of the laminae and the laminate, obtained by CLT (Classical lamination ´theory) by using the software ESACOMP, are given at Table 1 and 2, respectively.

- CYCOM 977-2 is an advanced resin system, which comes with intermediate modulus carbon fibers, to be processed in autoclave, but still able to produce good quality laminates under OOA (Out of Autoclave) conditions, as were used for this work.

A cocuring process was followed: Firstly, central laminates were cured and cut to the desired size, then the optical fibre was located at a small groove done on the surface, to fix its position and to avoid any movement.

A fresh adhesive film, FM300 (0,2 mm thickness, G = 0,907 GPa), was located onto it, an uncured laminate with the size of the upper adherent was added on top, a vacuum bag was done and the assembly was cured at an oven, with the prescribed cure cycle. (T = 180ºC, 2 hours)

As a second step the assembly was turned upside-down, and again a fresh adhesive layer was located onto it, and the ink with CNT was painted at the defined positions sketched at fig 2. It has been found that the adhesive has a significant flow under the curing conditions. Micrographs taken at previous works demonstrated that the carbon nanotubes penetrate the pure resin of the adhesive in contact with it, and also to the resin of the uncured prepreg, if located onto it. In order to get a higher reproducibility, linked to the final percentage of CNT into the cured resin, the optimal being near the percolation threshold, it was decided to cure the first layer of adhesive, then adding a second adhesive layer and the uncured laminate for the upper adherent. Note that the width of this laminate is slightly smaller than the central laminate, to make easier the installation of electrodes for the CNT strips.

Table 1: Material properties CYCOM 977-2

Moduli (GPa)		Poisson's ratios	
E_{11}	175,00	nu_{12}	0,3
E_{22}	8,68		
G_{12}	4,30		

Table 2: Laminate stiffness properties (Obtained by ESACOMP)

Laminate: Lay-up:$((0/90)_3/0)$SO h = 2.444 mm			
In plane Modulus (GPa)			
E_{xx}	98,60	nu_{xy}	0,0305
E_{yy}	85,76		
G_{xy}	4,30		

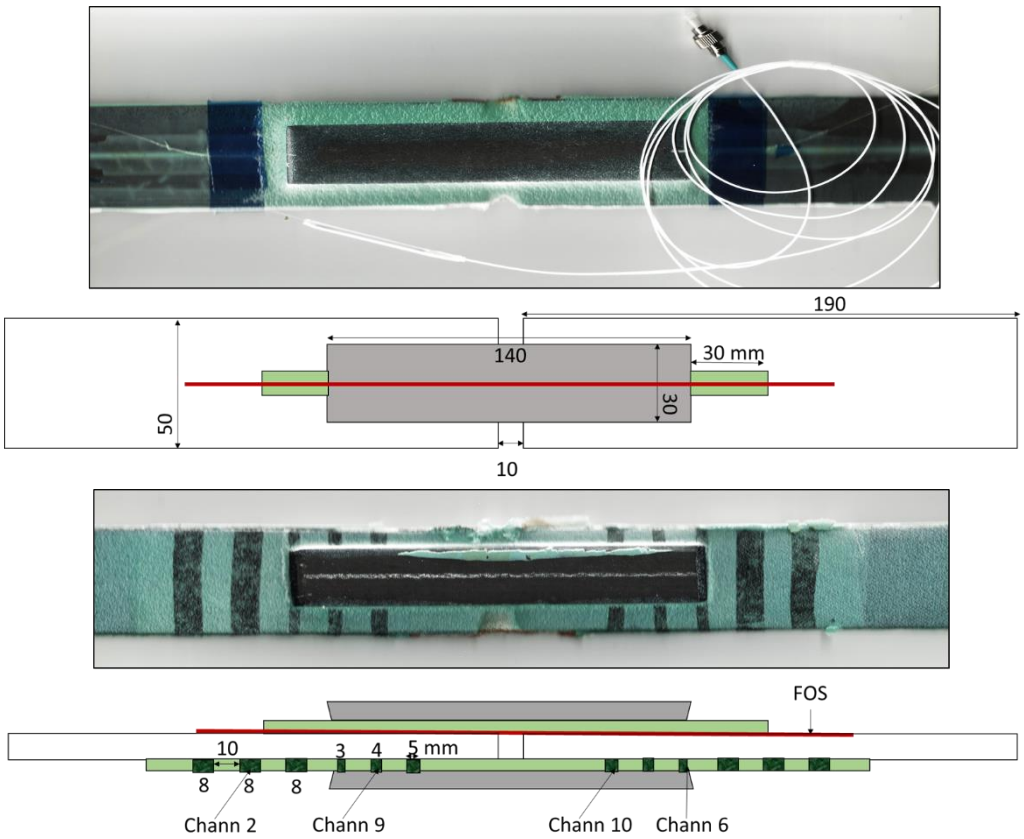

Figure 2 .Double lap bonded joint specimen

3. Theoretical and Experimental Results

3.1. Strain field predicted by the numerical models

The calculation for the strain field at the double lap bonded joint has been done with the software ESACOMP, which uses the CLT to model the response of the adherents (plain stress state for each lamina, the strain vary linearly through the laminate thickness), and the adhesive layer is modeled as distributed linear tension and shear springs. Further details can be found at the link [22].

The shear stress distribution for the bonded joint with the dimensions given at Fig 2, assuming clamped-clamped boundary conditions, for an external load of 100 kN/m (5 kN for an specimen width of 50 mm), are given at figure 3 (because of the symmetry of the specimen, results are represented for only a halve). As expected, the shear strain peaks at the end and the middle of the joint, this side slightly higher, because of its higher stiffness. These results are in good coincidence with those afforded by the Volkersen and Goland-Reissner analytical models.

According to these theories, the shear strain would be simply $\varepsilon_{xz}= \tau_{xz}/G_a$, uniform through the adhesive thickness, only dependent on x. For the axial strains, assuming valid the Volkersen hypothesis, the equilibrium equations for each adherent establish (Eq 1)

$$t\partial\sigma_1/\partial x = \tau \cdot \qquad (1)$$

being t the thickness of the adherent, σ the tensile stress at this point (related to the strain by $\sigma = E\,\varepsilon$) and τ the adhesive shear stress.

So, the shear stresses can be correlated with the axial strains at each interface, which are the same as the attached laminate.

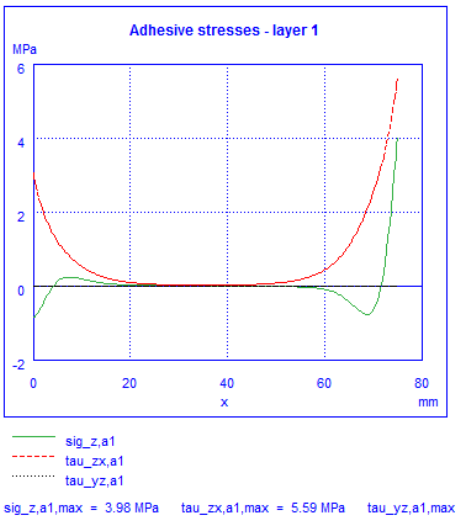

Figure 3 Calculated shear strains at the double lap joint, for an applied load of 100 kN (ESACOMP)

3.2. Tests results from distributed fiber optic sensors

Distributed strain measurements were done by an equipment OBR Luna 4600. Figure 4 gives the axial strain field obtained by the embedded optical fibre, attached to the central laminate. The response was linear with the applied load, only results for two load tests are given.

As mentioned above, a plain optical fibre, acrylate coated, was located at a small groove done at the surface of the laminate, before the adhesive was cured, so it is assumed that it gets the strains of the laminate. In fact, for the free region, outside the bonded joint, the measured strain for an applied load of 14,5 kN was 1250 με which is in good agreement with the calculated results for this laminate. Results predicted by ESACOMP for an applied load of 300 kN/m (15 kN for a specimen width of 50 mm) are:

- ε_{xx}= 1245 με, ε_{yy} = -390 με, ε_{xy} = 0

As justified at the former section, the spatial derivative of these axial strains should be coincident with the shear strain field. The derivative of experimental axial strains is also included at figure 4 (done as $\Delta\varepsilon/\Delta x$), but the agreement with the numerical shear strain field is only qualitative; it identifies the global trend, but the numerical values are not in agreement with calculations. It can be explained by two facts:

Firstly, the spatial resolution of OBR system is linked to the required strain accuracy; we choose 5 mm as a good trade-off. Secondly, it was recently demonstrated [23] that the coating of the optical fibre, which transfer the strains to the optical core, might have a shear lag effect, distorting the acquired strain field in case of large strain gradients.

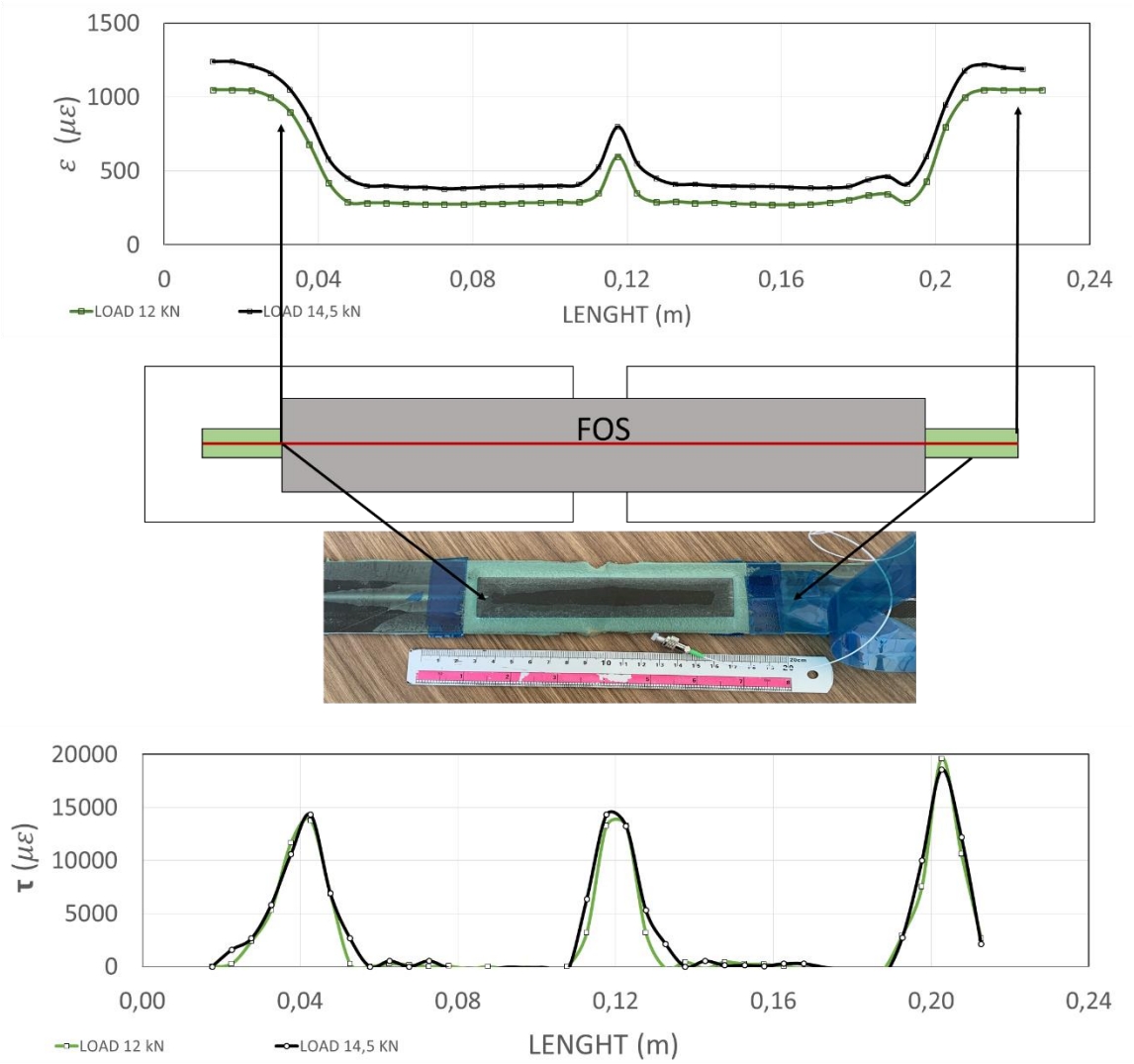

Figure 4 .Experimental axial strain (a) and calculated shear strains (b) at the double lap joint, for an applied load of 100 kN

3.3. Tests results from CNT doped films

The electrical resistance of the doped channels was acquired during the mechanical tests by an Agilent equipment. Some of the obtained results are presented at figure 6 and figure 7.

The first important conclusion is that the direction of the conductive strip does not influence the readings. In our case, the strips are transversally located, but the readings are mainly due to the longitudinal strains, that are responsible of a change among the distance of nanotubes. In fact, because of the isotropic distribution of nanotubes, the change of electrical resistance must be associated to what is called 'the hydrostatic strains' Equation (2),

$$3\varepsilon_{hyd} = \varepsilon_{11} + \varepsilon_{22} + \varepsilon_{33}, \quad (2)$$

Second conclusion is that, even the linearity of the response under increasing loads, it is difficult to get a quantitative response, because the gauge factor (ratio among the strain and the relative change of resistance) is not repetitive from a sensor to another one, being related to the dispersion of nanotubes into the adhesive.

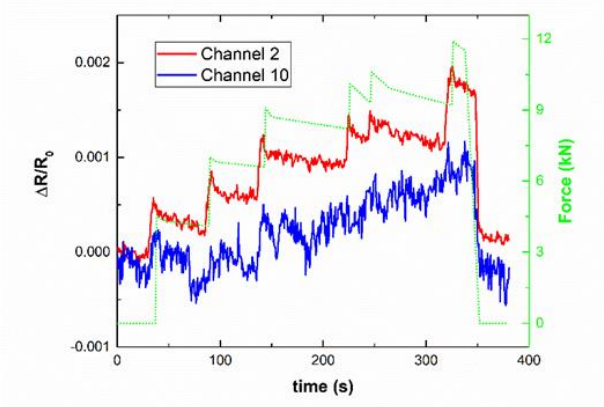

Figure 6 Electrical response as a function of the mechanical load for (a) Channels 2 and 10.

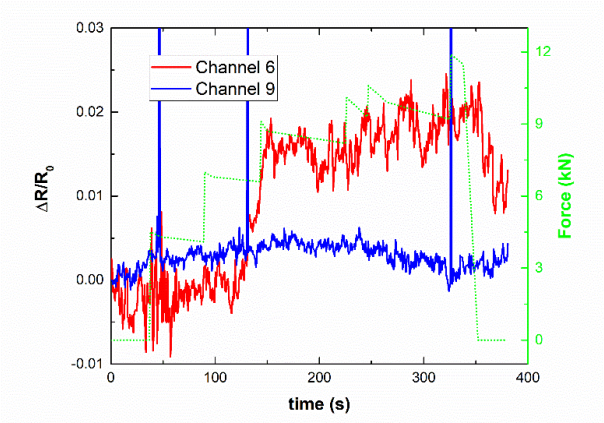

Figure 7 Electrical response as a function of the mechanical load for Channels 6 and 9.

4. Conclusions

The strain measurements inside a bonded joint have been successfully implemented by two different techniques. With distributed fiber optic sensors it has been found that strains can be quantitatively determined, except at the ends of the joint, because of the strong strain gradients.

Concerning carbon nanotubes thin films, it has been demonstrated its very high sensitivity to strains, and a very simple technique to implement local measurements, by using a CNT-ink, has been demonstrated. It has been found the lack of directionality of the CNT sensors, and at least in our experiments, the difficulty to obtain a nearly uniform gauge factor.

Acknowledgements

For authors of the first Institution, this work has received partial support from the DACOMAT Project. The DACOMAT project has received funding from the European Union's Horizon 2020 research and innovation programme under GA No. 761072.

References

[1] S.Budhe, M.D.Banea S.de Barros, L. F.M.da Silva, An updated review of adhesively bonded joints in composite materials, Int J Adhes Adhes, 72 (2017), pp. 30-42

[2] L.F.M. da Silva, P.J.C. das Neves, R.D. Adams, J.K. SpeltAnalytical models of adhesively bonded joints—Part I: literature survey Int J Adhes Adhes, 29 (2009), pp. 319-330

[3] M.P. Moutrille, K. Derrien, D. Baptiste, Xavier Balandraud, Michel Grediac. Through-thickness strain field measurement in a composite/aluminium adhesive joint. *Composites Part A: Applied Science and Manufacturing*, Elsevier, 2008, pp. ⟨ hal-00311871⟩

[4] A.J.Comer, K.B.Katnam, W.F.Stanley,T.M.Young . Characterising the behaviour of composite single lap bonded joints using digital image correlation. Int J Adhes, 40 (2013), pp. 215-223

[5] M.Y. Tsai, J. Morton., An investigation into the stresses in double-lap adhesive joints with laminated composite adherends, International Journal of Solids and Structures 47 (2010) 3317–3325

[6] A. Guemes; S. Diaz-Carrillo; J. M. Menendez, Measurement of strain distribution in bonded joints by fiber Bragg gratings. Volume 3330, Smart Structures and Materials 1998:

[7] L Canal, et al., Monitoring strain gradients in adhesive composite joints by embedded fiber Bragg grating sensors. Composite Structures 112 (2014) 241–247

[8] Childers, B.A., Froggatt, et al. (2001). Use of 3000 Bragg grating strain sensors distributed on four eight-meter optical fibers during static load tests of a composite structure. Proc. SPIE, 4332, 133-142

[9] H Murayama, et al., Strain monitoring of a single-lap joint with embedded fiber-optic distributed sensors

[10] A. Güemes, A. Fernández-López, et al., Structural Health Monitoring in Composite Structures by Fiber-Optic Sensors. Sensors, Vol 18, N4 (2018)
[11] Takeda, N., Minakuchi, S.Life cycle monitoring and quality control of aerospace composite structures (2016) 8th European Workshop on Structural Health Monitoring, EWSHM 2016, 2, pp. 1479-1486.
[12] Tur, M., Ben Simon, U., Gorbatov, N., Bergman, A., Kressel, I., Kontis, N., Koimtzoglou, C. Impact damage detection for composite fuselage panel using distributed strain sensing based on fiber optic Rayleigh back-scattering (2016) IACAS 2016 - 56th Israel Annual Conference on Aerospace Sciences, .
[13] Murayama, H., Ning, X., Kageyama, K., Wada, D., Igawa, H. Dynamic measurement of inside strain distributions in adhesively bonded joints by embedded fiber Bragg grating sensors (2014) Proceedings of SPIE - The International Society for Optical Engineering, 9157
[14] A. Güemes, SHM technologies and applications in aircraft structures 5th Inttnal Symposium on NDT in Aerospace, Singapore, Vol 13-15, 2013.
[15] Ning Xiaoguang, Structural health monitoring of adhesive bonded single-lap joints in composite materials by fiber-optic distributed sensing system. PhD dissertation, University of Tokyo, (2013)
[16] Alamusi, et al., Piezoresistive Strain Sensors Made from carbon nanotubes based polymer nanocomposite Sensors 2011, 11, 10691-10723
[17] Waris Obitayo and Tao Liu. , A Review: Carbon Nanotube-Based Piezoresistive Strain Sensors. Journal of Sensors, (2012)
[18] Han Zhang, Emiliano Bilotti & Ton Peijs (2015) The use of carbon nanotubes for damage sensing and structural health monitoring in laminated composites: a review, Nanocomposites, 1:4, 167-184, DOI: 10.1080/20550324.2015.1113639
[19] Olfa Kanoun et al., Flexible Carbon Nanotube Films for High Performance Strain Sensors. Sensors 2014, 14, 10042-10071; doi:10.3390/s140610042
[20] Y. Zhao, et al., In situ strain monitoring of a single lap joint using inkjet-printed CNT embedded thin films. IJSHM Vol 18 (5-6), (2019)
[21] XF Sánchez-Romate,et al., Development of bonded joints using novel CNT doped adhesive films: Mechanical and electrical properties. Innttnal J. Adhesion and Adhesives 86, (2018)
[22] F. Mortensen, Theoretical background of ESACOMP analysis,https://altairuniversity.com/wp-content/uploads/2018/06/5-joints.pdf
[23] U. Ben-Simon, et al., Choosing the right Optical Fiber coating to meet individual Fiber-optic strain measurement applications. Proceedings IWSHM 2019 , Stanford, (2019)